The evolution from long-range magnetic order to spin-glass behaviour in $PrAu_2(Si_{1-x}Ge_x)_2$

A Krimmel, J Hemberger, C Kegler, M Nicklas, A Engelmayer, G Knebel, V Fritsch, M Reehuis†, M Brando and A Loidl

Experimentalphysik V, Elektronische Korrelationen und Magnetismus, Institut für Physik, Universität Augsburg, D-86159 Augsburg, Germany

Abstract. We have studied the magnetic behaviour of $PrAu_2(Si_{1-x}Ge_x)_2$ by means of magnetic susceptibility, resistivity, and heat capacity measurements, and x-ray and neutron powder diffraction. All compounds are isostructural and crystallize in the well known $ThCr_2Si_2$-type structure. $PrAu_2Si_2$ shows the characteristic features of a canonical spin glass with a freezing temperature of $T_F = 3$ K. Completely unexpectedly, on introducing/increasing the atomic disorder by alloying with Ge, the spin-glass transition is suppressed as is first evident from a slight decrease of the freezing temperature T_F up to $x = 0.10$. Long-range magnetic order sets in for $x \geqslant 0.12$. Within the range $0.15 \leqslant x \leqslant 1$, all compounds show the same simple AF-I-type antiferromagnetic structure with a monotonic increase of both the Néel temperature and the ordered magnetic moment for increasing Ge concentration. The magnetic phase diagram of $PrAu_2(Si_{1-x}Ge_x)_2$ is explained by the presence of weak disorder at a constant level at the Au sites. Clear indications of crystal-field effects have been observed.

1. Introduction

The ternary intermetallic compounds RT_2X_2 (R = rare-earth metal, T = transition metal, and X = Ge, Si) have been studied intensively during the past few decades. The large number of different compounds exhibiting this 1:2:2 stoichiometry together with the simple tetragonal symmetry and a rich variety of exciting magnetic properties is stimulating continuous research [1]. Many of these compounds order magnetically at low temperatures where usually only the rare-earth sublattice carries a magnetic moment [1]. Also more complex phenomena were found in many Ce and U compounds which reveal heavy-fermion (HF) and intermediate-valence behaviour including HF superconductivity [2]. For the praseodymium compounds, different types of magnetic order have been observed: $PrRu_2Si_2$ [3], $PrRu_2Ge_2$ [4], and $PrOs_2Si_2$ [5] show ferromagnetism, while the other compounds of this intermetallic series investigated so far order antiferromagnetically, displaying both complex ($PrCo_2Si_2$ [6] and $PrNi_2Si_2$ [7]) and simple collinear types of structure. $PrNi_2Si_2$ [8] is the prototype of an amplitude-modulated incommensurate structure owing to its singlet ground state, whereas $PrCo_2Si_2$ is a multi-step metamagnet and has been discussed as a candidate for displaying devil's staircase behaviour [9]. In all of these compounds crystal-field (CF) effects are essential in determining the magnetic behaviour. In this context, it has been speculated that $PrCu_2Si_2$ may be the first example of a Pr-based heavy-fermion compound displaying the multi-channel

Kondo effect [10, 11]. However, a detailed inelastic neutron scattering study favoured an explanation of the unusual behaviour of $PrCu_2Si_2$ in terms of CF wave functions only [12]. Recently, Süllow *et al* [13] discovered spin-glass (SG) behaviour in URh_2Ge_2. Since the necessary conditions for achieving a spin-glass ground state are frustration and disorder, the behaviour of URh_2Ge_2 is surprising. Usually, these intermetallics reveal a perfect periodic atomic arrangement leading to a structural stability over a very large temperature range with a strict stoichiometric ratio of 1:2:2. However, two different crystallographic structures are allowed for these compounds, differing only in their T and X positions. They crystallize either in the $ThCr_2Si_2$-type (space group $I4/mmm$) [14] or the $CaBe_2Ge_2$-type structure (space group $P4/nmm$) [15]. To explain the spin-glass behaviour observed in URh_2Ge_2, Süllow *et al* [13] proposed an amalgamation of these two structures, leading to a statistical distribution of the Rh and Ge positions. This in turn creates random bonds leading to competing magnetic interactions. Already some years ago, Gschneidner Jr *et al* [16] suggested the possible appearance of non-magnetic disorder spin glasses in Ce and U compounds. They argued that structural disorder around the f atoms causes a distribution of RKKY interactions, yielding a frustrated ground state due to random bonds. Concomitantly, SG behaviour and CF effects are responsible for the high values of the linear term of the specific heat and therefore these are often falsely interpreted as HF compounds [16]. The RAu_2Si_2 compounds were investigated previously by x-ray diffraction and magnetic susceptibility measurements down to 4.2 K [17, 18]. For $PrAu_2Si_2$, the susceptibility data [18] showed paramagnetic behaviour and the x-ray diffraction measurements revealed the $ThCr_2Si_2$-type structure. In particular, it has been reported that atomic disorder of the Au and Si atoms can be excluded [17, 18]. Recently, we have found spin-glass behaviour in $PrAu_2Si_2$ [19], another example of a fully stoichiometric compound without any intentionally introduced disorder. To study the effect of non-magnetic disorder, we report on measurements of the alloy series $PrAu_2(Si_{1-x}Ge_x)_2$ which exhibit a transition from spin-glass behaviour to long-range antiferromagnetic order.

2. Experimental details and results

Our samples have been synthesized by argon arc melting of the stoichiometric mixtures from commercially available high-purity (4N) elements. To assure homogeneity, the ingots were subsequently annealed for one week at $T = 1100$ K and characterized by their Guinier x-ray diffraction patterns using Cu Kα_1 radiation. All diffraction data were analysed by the standard Rietveld method [20] employing the FULLPROF program [21]. The x-ray diffraction pattern showed single-phase material in accordance with the fully ordered $ThCr_2Si_2$ type of structure throughout the whole concentration range and in agreement with the results of the early x-ray studies on $PrAu_2Si_2$ [17, 18].

Magnetic susceptibility measurements have been performed in an ac susceptometer in fields up to 14 T between 1.8 K and room temperature. The susceptibility data, as shown in figure 1, have been recorded at a measuring frequency of 113 Hz in a driving field of 0.2 G_{rms}. From the high-temperature Curie part of the susceptibility, the paramagnetic moments and the corresponding Curie–Weiss temperatures have been determined. For all compounds investigated the effective paramagnetic moment lies in the range 3.1 $\mu_B < \mu_{eff} < 3.5\ \mu_B$, compared to 3.58 μ_B for the free Pr^{3+} ion. The Curie–Weiss temperatures display an almost constant negative value of around $\Theta \approx -10$ K indicating antiferromagnetic interactions. A maximum of $\chi(T)$ in between 2 and 12 K (dependent on concentration) indicates a magnetic transition, as shown in figure 1. The magnetic properties of $PrAu_2(Si_{1-x}Ge_x)_2$ are summarized in table 1. For the silicon-rich compounds with $x \leqslant 0.1$, canonical spin-glass behaviour has been found, as is evident from:
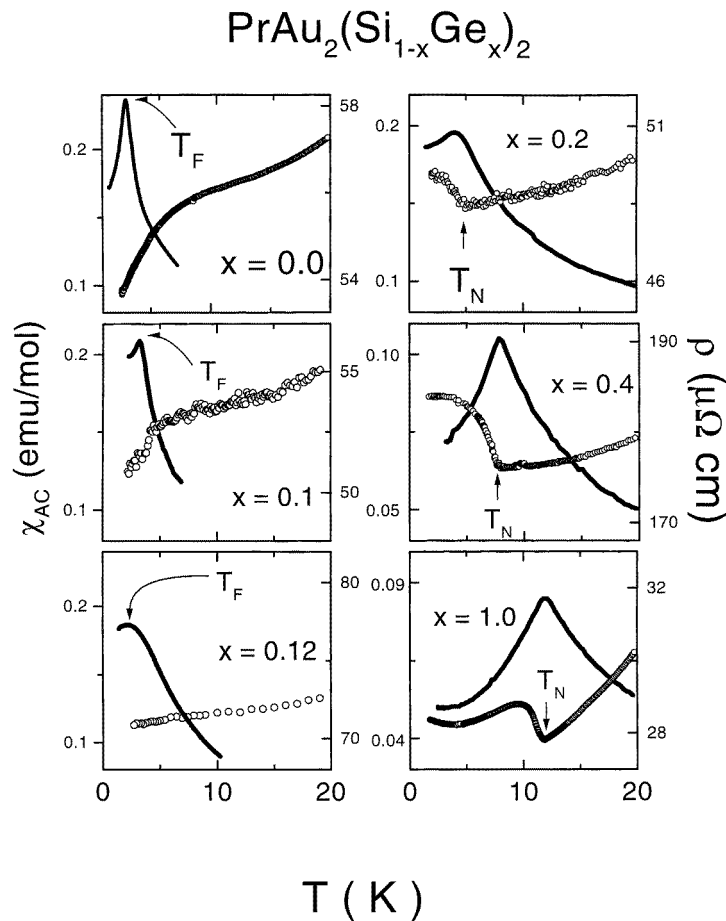
Figure 1. The temperature dependence of the magnetic susceptibility and resistivity of $PrAu_2(Si_{1-x}Ge_x)_2$. The susceptibility measurements have been performed at a measuring frequency of 113 Hz in a driving field of 0.2 G_{rms}. The transition temperatures T_N and T_F are indicated by arrows.

 (i) a maximum of $\chi(T)$ at around $T = 3$ K (compare with figure 1);
 (ii) the onset of irreversibility of the magnetization which in turn defines a quasi-static spin-glass freezing temperature T_F, as shown in the upper part of figure 2;
(iii) a weak frequency dependency of the maximum of the loss χ''_{ac} which corresponds to the inflection point of the real part χ'_{ac} typical for spin-glass systems [22], as illustrated in the lower part of figure 2 for the pure $PrAu_2Si_2$ and the 10% Ge-doped compound;
(iv) a strong increase (divergence) of the non-linear susceptibility (not shown here);
 (v) the relaxation of the isothermal remanance magnetization (IRM) following a stretched-exponential decay over several orders of magnitude in time.

The canonical spin-glass behaviour is further corroborated by the other experimental techniques as described below.

For $x = 0.12$ and higher Ge concentrations, the susceptibility measurements provided no further evidence for the onset of irreversibility of the magnetization and the maxima at the

Table 1. Magnetic properties of $PrAu_2(Si_{1-x}Ge_x)_2$: the antiferromagnetic ordering temperature T_N or the quasi-static freezing temperature T_F of the spin-glass (SG) state, as determined by magnetic susceptibility measurements (χ) or neutron diffraction (N.D.), respectively, the Curie–Weiss temperatures Θ, the effective paramagnetic moments μ_{eff}^{para} and the ordered magnetic moments μ_{ord}, the critical magnetic field B_c of the spin-flop transitions, and the reliability factors of the Rietveld refinement for the magnetic phase assuming the AF-I type of magnetic structure for $x \geqslant 0.12$.

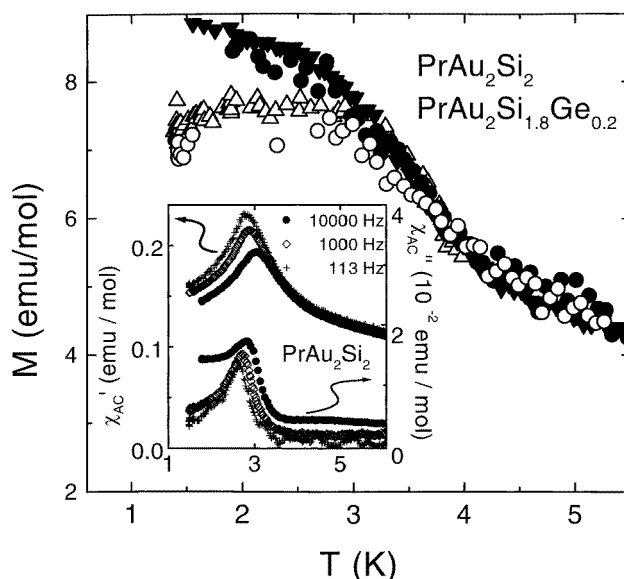| x	T_N or T_F (K) (χ/N.D.)	Θ (K)	μ_{eff}^{para} (μ_B)	μ_{ord} (μ_B)	B_c (T)	R_{mag} (%)	Type of magnetic order
1	11.9/11.6	−14.2	3.46	2.09(4)	3.1	6.08	AF-I
0.8	11.1/10.6	−13.6	3.38	2.33(4)	2.7	3.90	AF-I
0.6	10.0/9.5	−17.2	3.47	1.96(4)	2.4	4.57	AF-I
0.4	7.8/7.5	−8.3	3.30	1.75(3)	1.75	6.78	AF-I
0.2	4.0/4.0	−14.6	3.39	1.04(5)	1.0	8.33	AF-I
0.12	2.0/—	−10.4	3.09				SG
0	3.2/—	−14.6	3.53				SG

Figure 2. Field-cooled (FC) and zero-field-cooled (ZFC) magnetization of pure and 10% Ge-doped $PrAu_2Si_2$. Full symbols correspond to field-cooled, open symbols to zero-field-cooled magnetization curves. Triangles and circles are shown for pure $PrAu_2Si_2$ and 10% Ge-containing compounds, respectively. The onset of the irreversibility defines a quasi-static spin-glass freezing temperature T_F. The real and imaginary parts of the magnetic susceptibility of $PrAu_2Si_2$ for different frequencies are shown in the inset. The maximum of χ_{ac}'' corresponds to the inflection point of χ_{ac}', both representing $T_F(\nu)$. The small frequency shift of the freezing temperature is characteristic for spin-glass systems.

transition temperature become sharper. This is the first evidence of a change of the ground state from spin-glass behaviour to long-range magnetic order upon doping $PrAu_2Si_2$ with Ge above a critical Ge concentration of $x_c = 0.12$.

Additionally, magnetization measurements have been performed in magnetic fields up to 14 T for $x = 1, 0.8, 0.4$, and 0.2. As a characteristic feature of an antiferromagnet, a

spin-flop transition occurs in the presence of an applied magnetic field at a critical value of the field strength, which is reflected in the field dependence of the magnetization and the susceptibility, respectively. The field-dependent susceptibilities of $PrAu_2(Si_{1-x}Ge_x)_2$ are shown in figure 3. As an example, the inset of figure 3 displays the magnetization for $PrAu_2Ge_2$. In low magnetic fields the magnetization increases linearly (polycrystalline samples), then a steep increase reflects the spin-flop transition, followed again by a linear field dependence of the magnetization within the spin-canted phase in a moderate range of fields. At still higher fields, the magnetization starts to saturate. Within mean-field theory, the critical spin-flop field H_c of an antiferromagnet is determined by

$$H_c = \sqrt{H_A^2 + 2H_A H_{ex}}$$

where H_{ex} is the exchange and H_A the anisotropy field. The critical field may also be expressed in terms of the susceptibilities $\chi_\parallel$ and $\chi_\perp$ and an anisotropy constant K. Assuming an ideal Néel antiferromagnet, for which $\chi_\perp$ remains constant below T_N and $\chi_\parallel$ becomes zero at $T = 0$, and for an ideal polycrystalline sample where χ_{powder} is two-thirds of $\chi_\perp$, the characteristic fields can be calculated according to $H_{ex} = 11$ T and $H_A = 0.75$ T for pure $PrAu_2Ge_2$.
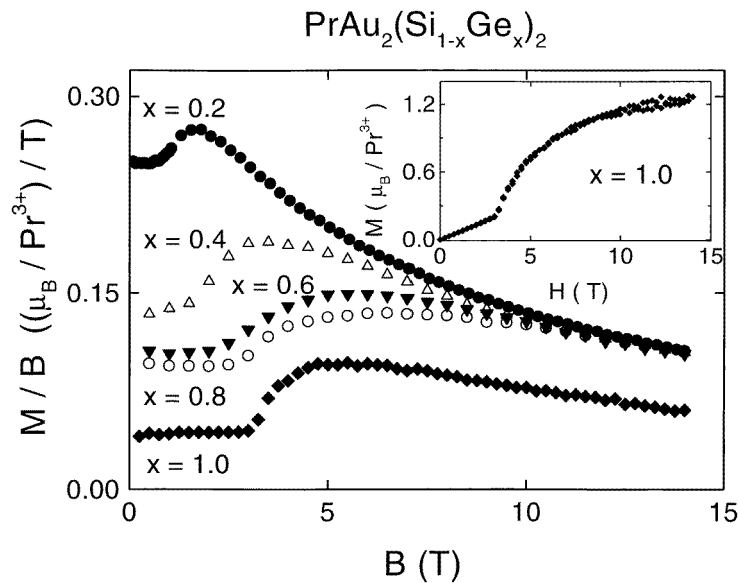

Figure 3. The susceptibility (M/B) of $PrAu_2(Si_{1-x}Ge_x)_2$ as a function of an applied magnetic field. The measurements for $x = 0.2$ (full circles) and $x = 0.4$ (open triangles) have been performed at $T = 2$ K, whereas the measurements for the compounds with $x = 0.6$ (full squares), $x = 0.8$ (open circles) and $x = 1$ (closed diamonds) were performed at $T = 5$ K. The inset shows the field-dependent magnetization of $PrAu_2Ge_2$ displaying a field-induced magnetic transition (spin flop) at a critical field of $B_c = 3.2$ T.

The difference between the magnetic transitions below and above the critical concentration of $x = 0.12$ is also reflected in the behaviour of the resistivity, which is included in figure 1. The electrical resistance experiments have been performed employing a conventional four-probe method for temperatures 1.5 K $\leqslant T \leqslant 300$ K. For $x \geqslant 0.15$ the maximum of the magnetic susceptibility at the transition temperature corresponds to a sharp increase in ρ, indicating the opening of a gap at the Fermi surface (or parts of it) at T_N. Such a behaviour is found in several rare-earth metals [23] and, remarkably, in the $Pr(Ni_{1-x}Cu_x)_2Si_2$ compounds [24].

The critical concentration $x = 0.12$ shows a linear dependence of the resistivity upon temperature (compare with figure 1), whereas below $x = 0.12$ the formation of a spin-glass state is reflected by a sudden decrease of the resistivity slightly above T_F (see again figure 1). Within the spin-glass regime, due to the competition of the RKKY and Kondo interaction, a peak in the 'magnetic part' of the resistivity is expected for $T > T_F$.

The results of the specific heat measurements employing a semi-adiabatic heat pulse technique are shown in figure 4. The data have been corrected for phonon contributions by means of measurements on the non-magnetic reference compounds $LaAu_2(Si_{1-x}Ge_x)_2$. For $PrAu_2Ge_2$ a pronounced λ-shaped anomaly at 11.5 K reflects the onset of long-range antiferromagnetic order. With increasing Si content this anomaly is shifted towards lower temperatures, becomes weaker, and is flattened out. For all concentrations except for pure $PrAu_2Ge_2$ the specific heat decreases above the magnetic transition temperature, passing through a minimum at around 15 K. As can be seen from figure 4, plotting C/T versus T^2, the high-temperature linear part extrapolated linearly towards $T = 0$ corresponds to moderately enhanced Sommerfeld coefficients $50 \leqslant \gamma \leqslant 100$ mJ mol^{-1} K^{-2}. The inset of figure 4 shows the magnetic entropy of $PrAu_2(Si_{1-x}Ge_x)_2$ as determined by integrating C/T over temperature. Just above the magnetic ordering temperatures, the value of the magnetic entropy reaches only about 50% of $R \ln 9$ (the corresponding Pr^{3+} free-ion value) and is close to $R \ln 3$. This points to a quasi-threefold-degenerate magnetic ground state.
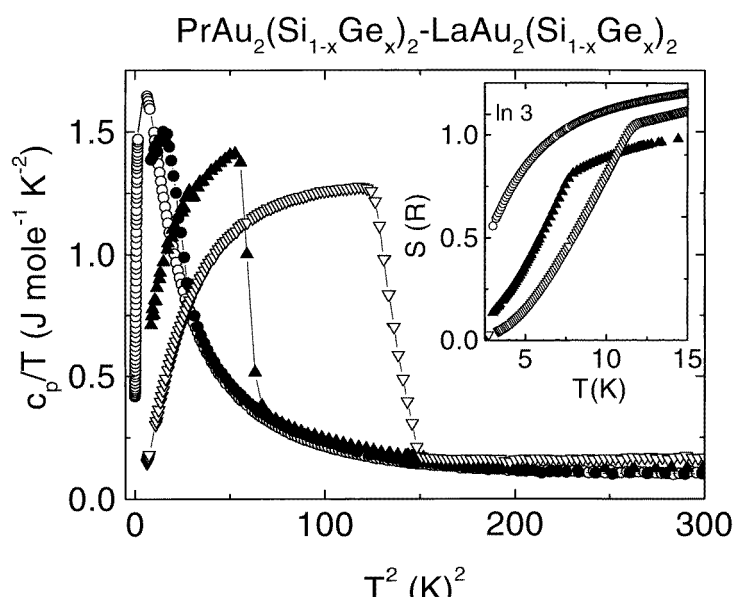

Figure 4. Specific heat c_p/T versus T^2 for $PrAu_2(Si_{1-x}Ge_x)_2$, corrected for phonon contributions by subtracting the heat capacity of the non-magnetic reference compounds $LaAu_2(Si_{1-x}Ge_x)_2$. The inset shows the corresponding magnetic entropies as determined by integrating c_p/T over temperature. Open circles corresponds to $x = 0$, closed circles to $x = 0.2$, closed triangles to $x = 0.4$, and open triangles to $x = 1$.

Neutron powder diffraction experiments have been performed on the diffractometer E6 at the Hahn Meitner Institut, Berlin. An incident wavelength of $\lambda = 2.45$ Å has been selected by a pyrolytic graphite monochromator. Higher-order contamination was suppressed by a graphite filter. The carefully powdered samples were used to fill Al containers and mounted in an

orange-type cryostat allowing for temperatures $1.5 \, K \leqslant T \leqslant 300 \, K$. Diffraction patterns of $PrAu_2(Si_{1-x}Ge_x)_2$ were recorded between 1.5 and 20 K for $x = 0, 0.12, 0.2, 0.4, 0.6, 0.8$, and 1. In a first step, the nuclear intensities could be successfully refined assuming the fully ordered $ThCr_2Si_2$-type structure for all compounds investigated. For the Rietveld analysis, eleven parameters have been refined: the scale factor, zero point, lattice constants a and c, position parameter z, four profile function parameters, occupancies (or concentration, respectively), and the ordered magnetic moment. The unit-cell volume as a function of concentration is displayed in the upper part of figure 5. A linear increase with increasing Ge concentration is observed in the range $0.2 \leqslant x \leqslant 1$, whereas the unit-cell volume remains at an almost constant value for $0 \leqslant x \leqslant 0.2$. In the lower part of figure 5, the Pr–Au and Pr–Ge/Si ionic distances are shown for varying Ge/Si concentration. As is evident from this figure, the Pr–Au distance reveals a similar concentration dependence to the unit-cell volume, but the Pr–Ge/Si distance shows a completely different behaviour. This is a first hint that the Pr–Au distances may play an important role on the magnetic behaviour of $PrAu_2(Si_{1-x}Ge_x)_2$. The position parameter z of the Si or Ge ions was constant throughout the whole concentration range. The crystallographic data for $PrAu_2(Si_{1-x}Ge_x)_2$ resulting from the Rietveld refinement of the powder neutron diffraction experiments are summarized in table 2.
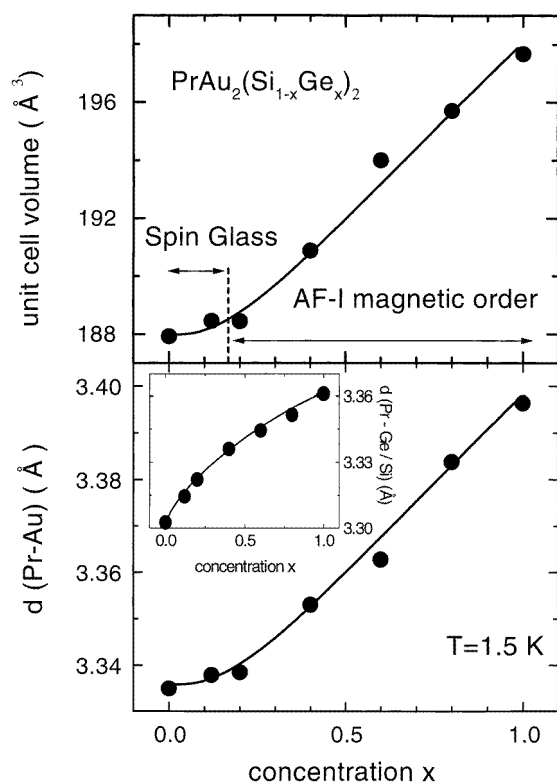

Figure 5. The unit-cell volume of $PrAu_2(Si_{1-x}Ge_x)_2$ (upper part) and Pr–Au and Pr–Ge/Si interatomic distances (lower part) as determined from the results of the refinement of the powder neutron diffraction data. Full curves are only to guide the eye.

The compounds $PrAu_2(Si_{1-x}Ge_x)_2$ with $x = 0.2, 0.4, 0.6, 0.8$, and 1 showed additional superlattice reflections in between the nuclear Bragg peaks at low temperatures, thus indicating the onset of long-range antiferromagnetic order. The low-temperature data could be successfully refined by assuming the simple collinear AF-I-type structure for all compounds with $x \geqslant 0.2$. As an example, the diffraction pattern for $x = 0.8$ is shown in figure 6 for $T = 20 \, K$

Table 2. Crystallographic data for $PrAu_2(Si_{1-x}Ge_x)_2$ resulting from the Rietveld refinement of the powder neutron diffraction experiments for $T = 1.5$ K when including site disorder between Au and Ge/Si (see the text). Lattice constants a and c, the fractional coordinate of the position parameter z of the Ge/Si ions, the occupancy and the corresponding Si concentration in %, the site disorder between Au and Ge/Si in %, and R_{Bragg} and R_F, the reliability factors of the Rietveld refinement, in %.

x	a (Å)	c (Å)	z	Occupancy/concentration (%) (Si)	Site disorder (%)	R_{Bragg}/R_F (%)
1	4.3538(3)	10.428(1)	0.386(1)	1	9.2	2.63/2.54
0.8	4.3414(4)	10.383(1)	0.386(1)	0.023(2)/18.5	7.0	4.88/3.80
0.6	4.3321(4)	10.341(2)	0.386(1)	0.049(3)/39.2	10.7	4.22/2.98
0.4	4.3101(3)	10.275(1)	0.387(2)	0.070(1)/56.3	10.9	3.29/2.50
0.2	4.2922(4)	10.229(2)	0.387(6)	0.093(3)/74.4	11.7	6.99/5.06
0.12	4.2934(5)	10.224(2)	0.386(1)	0.106(2)/84.8	11.0	4.63/3.59
0	4.289(1)	10.216(1)	0.385(3)	0	10.4	5.02/3.59

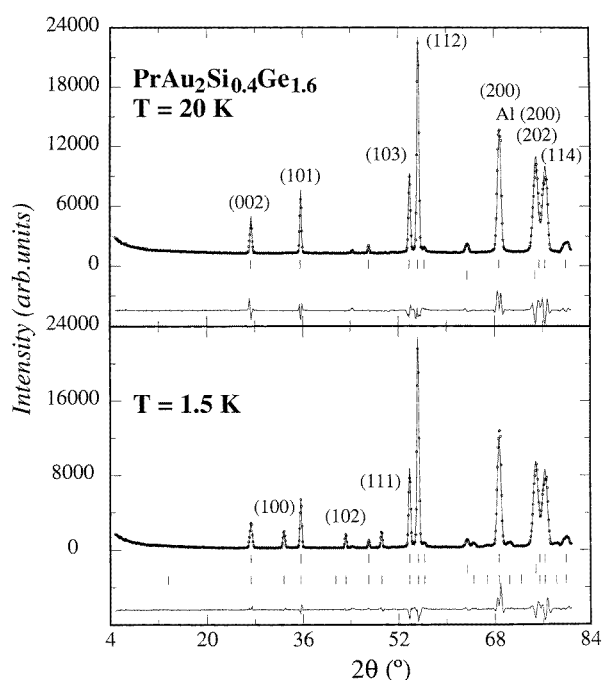**Figure 6.** Measured and calculated neutron diffraction patterns for $PrAu_2$ $(Si_{0.8}Ge_{0.2})_2$ at $T = 20$ K within the paramagnetic state (upper part) and at $T = 1.5$ K in the magnetically ordered state (lower part). The difference between the measured and calculated intensities is shown by the solid curve below the diffraction patterns. The angular positions of the Bragg peaks are indicated by vertical bars for the three fitted phases: $ThCr_2Si_2$-type structure for $PrAu_2$ $(Si_{0.8}Ge_{0.2})_2$ (uppermost vertical bars), Al to account for scattering of the container (second), and, for the low-temperature diffraction patterns only, the antiferromagnetic AF-I type of structure (lower vertical bars). The strongest crystallographic (upper part) and purely magnetic (lower part) Bragg peaks are indexed.

within the paramagnetic state and at $T = 1.5$ K in the magnetically ordered state, respectively. No magnetic Bragg peaks could be observed for $x = 0.12$ and the pure $PrAu_2Si_2$, revealing the absence of long-range magnetic order (more correctly, the absence of magnetic Bragg peaks is equivalent to an upper limit of the ordered magnetic moment of 0.25 μ_B). Starting

from $PrAu_2Ge_2$ a monotonic decrease of both the Néel temperature and the ordered magnetic moment is observed with increasing Si concentration. By subtracting the high-temperature (paramagnetic) from the low-temperature (magnetically ordered) intensities, the reflections of magnetic origin can be separated from the nuclear Bragg peaks. By monitoring the intensities of these magnetic reflections for varying temperature, the Néel temperatures and the temperature dependencies of the ordered magnetic moments have been determined for $x = 0.2, 0.4, 0.6, 0.8$, and 1. The values of the ordering temperatures are in good agreement with the values as determined by the magnetic susceptibility measurements. As regards the temperature dependence of the ordered magnetic moment, we first tried to fit the reduced values of the ordered moment $\mu_{ord}(T)/\mu_{ord}(T = 1.5 \text{ K})$ versus the reduced temperature T/T_N with a Brillouin function with $J = 4$ corresponding to the free Pr^{3+} ion. It can be seen from figure 7 that the experimentally determined values of the normalized magnetic ordered moments were always larger than the calculated values of the $J = 4$ Brillouin function for all concentrations investigated, exhibiting long-range magnetic order. Such a behaviour is a characteristic sign of the presence of crystal-field (CF) effects. As shown in figure 7, a good agreement between calculated and measured magnetic intensities is achieved by a fit employing a $J = 1$ Brillouin function. This points towards a threefold- (quasi-) degenerate ground state in $PrAu_2(Si_{1-x}Ge_x)_2$ throughout the whole concentration range, as suggested also on the basis of the specific heat measurements. The magnetic data for $PrAu_2(Si_{1-x}Ge_x)_2$ as determined by magnetic susceptibility measurements and the Rietveld refinements of the powder neutron diffraction data are summarized in table 1.
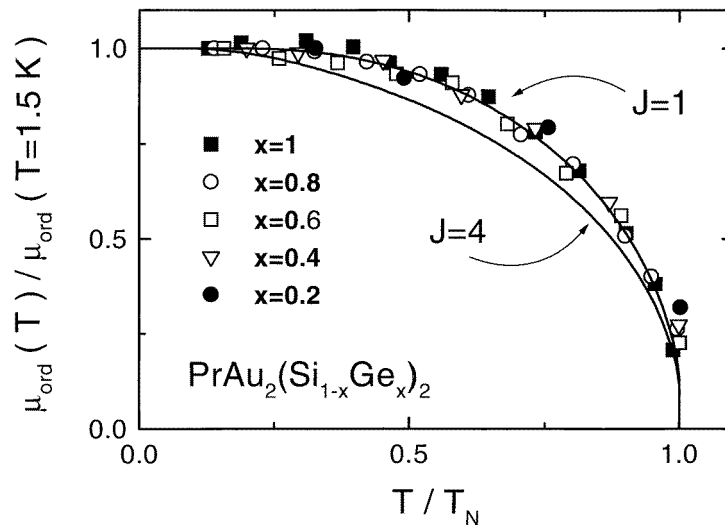

Figure 7. The normalized ordered magnetic moment $\mu_{ord}(T)/\mu_{ord}(T = 1.5 \text{ K})$ versus the normalized temperature T/T_N of $PrAu_2(Si_{1-x}Ge_x)_2$, fitted by a $J = 1$ Brillouin function (solid curve). For comparison, a $J = 4$ Brillouin function corresponding to a Pr^{3+} free ion is also shown.

3. Discussion and conclusions

The magnetic properties of $PrAu_2(Si_{1-x}Ge_x)_2$ have been studied by means of powder x-ray and neutron diffraction, magnetic measurements, and heat capacity and electrical resistance

experiments. The results may be summarized in a magnetic phase diagram that is shown in figure 8. Starting from $PrAu_2Ge_2$, a simple AF-I-type antiferromagnet with $T_N = 11.5$ K and an ordered magnetic moment of $\mu_{ord} = 2\ \mu_B$, the substitution of Si for Ge leads to a monotonic reduction of both the ordering temperature and the ordered magnetic moment. Such a behaviour is not unexpected. Despite the introduction of non-magnetic atomic disorder by the statistical distribution of Ge and Si, the fully ordered $ThCr_2Si_2$ type of crystallographic structure is preserved over the whole composition range and the unit-cell volume decreases linearly with increasing Si concentration up to 80% Si. The magnetic properties of the RT_2X_2 (R = rare-earth metal, T = transition metal, X = Ge, Si) compounds are dominated by the RKKY interaction and CF effects. The decrease of the ordering temperature and the ordered magnetic moment may be straightforwardly explained by a suitable CF level scheme. A similar behaviour is observed for the isotypic $PrFe_2X_2$ (X = Ge, Si) compounds [25]. These two iron homologues display an AF-II-type antiferromagnetic structure at low temperatures, whereas the values of the ordering temperature and the ordered magnetic moment are two times as large for $PrFe_2Ge_2$ as in $PrFe_2Si_2$ [25]. This difference is explained in reference [25] within the framework of a CF model. The $J = 4$ Hund's rule multiplet of the Pr^{3+} ion is split in a tetragonal environment into three doublets and five singlets. It was shown in reference [25] that the relative position of the $\Gamma_{t5}^{(1)}$ CF doublet plays a crucial role for the actual value of the ordered magnetic moment and T_N. Like in $PrFe_2X_2$, the c-axis is the easy direction in $PrAu_2(Si_{1-x}Ge_x)_2$, which points towards a negative sign of the CF parameter B_2^0. The presence of CF effects is also reflected in the specific heat and the susceptibility data, though neutron spectroscopic measurements are needed to determine the CF wave functions. The magnetic entropy as determined by integrating the specific heat over temperature reaches only about 50% of $R \ln 9$ at $T = 15$ K, thus being close to a value of $R \ln 3$. This points
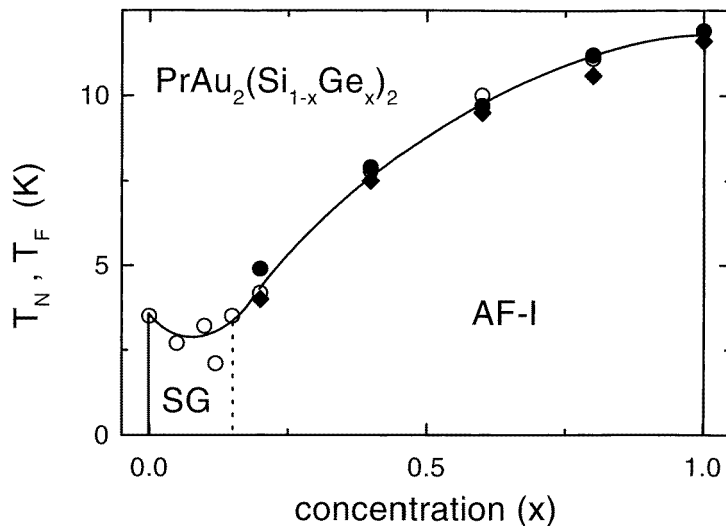

Figure 8. The magnetic phase diagram of $PrAu_2(Si_{1-x}Ge_x)_2$ obtained on the basis of the magnetic transition temperatures T_N (antiferromagnetic ordering temperature) for $x \geqslant 0.12$ and T_F (spin-glass freezing temperature at 113 Hz measuring frequency) for the Si-rich compounds. The symbols correspond to the maximum of $\chi(T)$ (open circles for both T_N and T_F), the minimum of ρ (full circles), and vanishing magnetic Bragg peaks in the neutron diffraction data (full diamonds). The solid curve is only a guide to the eye.

towards a (quasi-) threefold-degenerate ground state. This result is also in accordance with the temperature dependence of the ordered magnetic moment, which could be fitted by a $J = 1$ Brillouin function (compare with figure 7) whereas significant deviations have been observed assuming a $J = 4$ Pr^{3+} free-ion value.

The Fermi vector and therefore the RKKY interaction strongly depend on the a/c ratio and the number of free electrons. It should be noted that the simple AF-I type of magnetic structure in $PrAu_2(Si_{1-x}Ge_x)_2$ is *not* in agreement with the systematics of the RET_2X_2 compounds. On the basis of the a/c ratios [1], oscillatory complex magnetic order is expected to occur for $a/c \leqslant 0.415$ whereas simple antiferromagnetic structures should be stabilized in the opposite case. (In reference [25], a slightly different critical a/c ratio of $1/\sqrt{6} = 0.4082$ has been cited, also relying on reference [1].) The a/c ratio of $PrAu_2(Si_{1-x}Ge_x)_2$ between 0.418 and 0.420 is almost constant throughout the whole concentration range. Since it would be surprising to find a qualitatively different CF level scheme on going from $PrAu_2Ge_2$ to $PrAu_2Si_2$, and with an almost constant a/c ratio in mind, an overall identical magnetic behaviour is expected for $PrAu_2(Si_{1-x}Ge_x)_2$. Within the composition range of long-range antiferromagnetic order, the critical field of the spin-flop transition increases with increasing Ge concentration. When considering the critical field per ordered magnetic moment, an almost 50% increase of this B_c/μ_{ord} ratio is observed on going from $x = 0.2$ to $x = 1$. The same kind of behaviour holds for the T_N/μ_{ord} ratio. This reflects an increasing anisotropy for increasing Ge concentration which additionally stabilizes the magnetic order. It also demonstrates again the presence of CF effects in $PrAu_2(Si_{1-x}Ge_x)_2$.

The formation of a spin-glass state for $x \leqslant 0.12$, in particular in the case of the fully stoichiometric $PrAu_2Si_2$ compound, is very unusual. To explain the spin-glass behaviour observed in URh_2Ge_2, Süllow *et al* [13] proposed an amalgamation of the two possible structures allowed for 1:2:2 intermetallics, namely the $ThCr_2Si_2$ type (space group I4/mmm) [14] and the $CaBe_2Ge_2$ type of structure (space group P4/nmm) [15]. This leads to a statistical distribution of the Rh and Ge positions and in turn should create random bonds leading to competing magnetic interactions.

To explore the origin of the SG state we searched for disorder of Au and Si/Ge. Already, the low resistivity ratio $\rho(T = 300 \text{ K})/\rho(T = 1.7 \text{ K}) \approx 2$ as well as the rather high value at room temperature $\rho(T = 300 \text{ K}) = 140 \ \mu\Omega$ cm point to the presence of disorder in the spin-glass compound $PrAu_2Si_2$. A statistical distribution of Au and Si/Ge atoms among the 4(d) and 4(e) sites of the $ThCr_2Si_2$ type of structure most strongly affects the intensity of the (112) reflection, but only slightly affects the intensity of the (200) reflection. Hence, we calculated the experimentally observed intensity ratio $I_{(112)}/I_{(200)}$ and compared it to the ratio for the ideal $ThCr_2Si_2$ type of structure. From these values we determined a significant fraction of approximately 10% of our samples displaying disorder between Au and Si/Ge. This level of disorder remains constant over the whole composition range. This conclusion is confirmed by a more detailed Rietveld refinement. As is evident from figure 6, the peaks in the low angular range $4° \leqslant 2\Theta \leqslant 60°$ are rather well fitted in contrast to those in the high angular range $60° \leqslant 2\Theta \leqslant 84°$ where the largest differences between observed and calculated intensities are observed (compare with figure 6). Indeed, when only refining the diffraction pattern up to $2\Theta \leqslant 60°$, the residual R-value immediately drops down to 1.5–2%. The strongest deviation between observed and calculated intensities occurs for the (200) reflection at $2\Theta = 68°$. Interestingly, this (200) reflection is the only strong peak with $l = 0$ and is also the only strong peak of the diffraction pattern where the observed intensity is significantly stronger than the calculated one. The difference of the two crystallographically allowed structures for the 1:2:2 compounds is in the stacking sequence along c. Therefore an amalgamation of the $ThCr_2Si_2$ and the $CaBe_2Ge_2$ structure, as first proposed by Süllow *et al*

[13] for URh_2Ge_2, will not change the intensity of the (200) Bragg peak, but will lead to a decrease of intensity for $l \neq 0$ reflections. To confirm our conclusion beyond the argument of the intensity ratio, in a further step we performed again the Rietveld refinement with an increased scale factor to reach the amplitude of the (200) reflection while decreasing the intensities of the $l \neq 0$ reflections by allowing explicitly for a statistical distribution between the Au and Ge/Si sites. This leads to a stable refinement with slightly improved R-values as compared to the residuals when assuming the $ThCr_2Si_2$ structure only. The refined values of the site disorder are included in table 2 together with other crystallographic data for $PrAu_2(Si_{1-x}Ge_x)_2$. From the concentration dependence of the unit-cell volume and the interatomic distances as shown in figure 5 we know that for low Ge concentrations within the spin-glass regime the Pr–Au distance remains almost constant, whereas for higher Ge concentration long-range antiferromagnetic order evolves as soon as the unit-cell volume starts to expand. The simple AF-I type of magnetic structure is preserved irrespective of the degree of non-magnetic disorder on the Si/Ge sites. We therefore propose the following scenario to explain the phase diagram of $PrAu_2(Si_{1-x}Ge_x)_2$: in pure $PrAu_2Si_2$ the RKKY interaction tends to favour the formation of a long-range magnetically ordered ground state. The non-magnetic disorder between Au and Si ions leads to a statistical distribution of RKKY interactions around the Pr ions with a mean value J_0^{RKKY} and a width ΔJ^{RKKY}. Though the level of disorder of approximately 10% can be considered as a weak disorder, evidently it is sufficient to establish a spin-glass state. Since this level of disorder remains constant throughout the whole concentration range this is equivalent to a constant width ΔJ^{RKKY} of the distribution of RKKY interactions. For low Ge concentration up to 15% Ge, the unit-cell volume and in particular the Pr–Au distance remain constant, equivalent to a constant mean value J_0^{RKKY} of the RKKY interaction. Consequently, the spin-glass state is not altered for $0 \leqslant x \leqslant 0.12$. For higher Ge concentrations, the unit cell starts to expand and the Pr–Au distance becomes larger, leading to an increase of the mean RKKY interaction J_0^{RKKY}. As long as $\Delta J^{RKKY} \geqslant J_0^{RKKY}$ a spin-glass ground state is realized, in contrast to the case for $\Delta J^{RKKY} \leqslant J_0^{RKKY}$ where long-range magnetic order is established. This mechanism is independent of the degree of disorder on the Si/Ge sites. The Pr–Au distance determining the strength of the magnetic interactions and the weak but constant disorder on the Au sites is responsible for the different magnetic ground states in $PrAu_2(Si_{1-x}Ge_x)_2$. This explains why a spin-glass state in pure $PrAu_2Si_2$ is suppressed and replaced by an ordered state upon there being an overall increasing atomic disorder, but on the Ge/Si sites. The crucial disorder on the Au sites may indeed be expressed in terms of an amalgamation of the two different crystallographically allowed structures as proposed by Süllow *et al* [13] to explain the spin-glass behaviour found in URh_2Ge_2.

To conclude, we have studied the transition from long-range magnetic order to spin-glass behaviour in $PrAu_2(Si_{1-x}Ge_x)_2$. $PrAu_2Si_2$ is another example of a fully stoichiometric compound displaying a spin-glass ground state without any intentionally introduced disorder. Upon introducing/increasing atomic disorder by the substitution of Ge, the spin-glass state is first suppressed and then replaced by a simple AF-I-type antiferromagnetic order. The increase of the ordered magnetic moment and the ordering temperature is attributed to CF effects. The spin-glass formation is explained by non-magnetic disorder on the Au sites which remains at a constant and low level of about 10% for all concentrations. The overall magnetic behaviour, i.e. the phase diagram of $PrAu_2(Si_{1-x}Ge_x)_2$, is then determined by the competition of the disorder, characterized by the width ΔJ^{RKKY} of the distribution of RKKY interactions, and the mean value J_0^{RKKY} of the magnetic exchange. The crucial disorder on the Au sites may be expressed in terms of an amalgamation of the two different crystallographically allowed structures as proposed by Süllow *et al* [13].

Acknowledgments

References

[1] For a review, see for example
   Szytuła A and Leciejewicz J 1989 *Handbook on the Physics and Chemistry of the Rare Earths* vol 12, ed K A Gschneidner Jr and L Eyring (Amsterdam: Elsevier Science) p 133
[2] For review, see for example
   Grewe N and Steglich F 1991 *Handbook on the Physics and Chemistry of the Rare Earths* vol 14, ed K A Gschneidner Jr and L Eyring (Amsterdam: Elsevier Science) p 343
   Stewart G R 1984 *Rev. Mod. Phys.* **56** 755
[3] André G, Bourrée-Vigneron F, Oleś A and Szytuła A 1990 *J. Magn. Magn. Mater.* **86** 387
[4] Szytuła A, Oleś A, Perrin M, Kwok W, Sungaila Z and Dunlap B D 1987 *J. Magn. Magn. Mater.* **69** 305
[5] Hiebl H, Horvath C, Rogl P and Sienko M J 1983 *Solid State Commun.* **48** 211
[6] Nojiri H, Uchi M, Watamura S, Motokawa M, Kawai H and Endoh Y 1991 *J. Phys. Soc. Japan* **60** 2380
[7] Barandiaran J M, Gignoux D, Schmitt D, Gomez Sal J C and Rodriguez Fernandez J 1987 *J. Magn. Magn. Mater.* **69** 61
[8] Blanco J A, Gignoux D and Schmitt D 1992 *Phys. Rev.* B **45** 2529
[9] Takeda K, Konishi K, Deguchi H, Iwata N and Shigeoka T 1991 *J. Phys. Soc. Japan* **60** 2538
[10] Sampathkumaran E V and Das I 1993 *Physica* B **186–188** 328
[11] Sampathkumaran E V, Das I, Vijayaraghavan R, Hirota K and Ishikawa M 1991 *Solid State Commun.* **78** 971
[12] Goremychkin E A, Osborn R and Muzychka A Y 1994 *Phys. Rev.* B **50** 13 863
[13] Süllow S, Nieuwenhuys G J, Menovsky A A, Mydosh J A, Mentik S A M, Mason T E and Buyers W J L 1997 *Phys. Rev. Lett.* **78** 354
   Nieuwenhuys G J, Süllow S, Menovsky A A, Mydosh J A, Heffner R H, Le L P, MacLaughlin D E, Bernal O O and Schenk A 1998 *J. Magn. Magn. Mater.* **177–181** 803
[14] Ban Z and Sikirica M 1964 *Acta Crystallogr.* **18** 594
[15] Eisenmann B, May N, Müller W and Schäfer H 1972 *Z. Naturf.* b **27** 1155
[16] Gschneidner K A Jr, Tang J, Dhar S K and Goldman A 1990 *Physica* B **163** 507
[17] Felner I 1975 *J. Phys. Chem. Solids* **36** 1063
[18] Mayer I, Cohen J and Felner I 1973 *J. Less-Common Met.* **30** 181
[19] Krimmel A, Hemberger J, Nicklas M, Knebel G, Trinkl W, Brando M, Fritsch V and Loidl A 1999 *Phys. Rev.* B **59** R6604
   Hemberger J, Krimmel A, Nicklas M, Knebel G, Paraskevopoulos M, Trinkl W, Brando M, Fritsch V and Loidl A 1999 *Physica* B **259–261** 907
[20] Rietveld N 1969 *J. Appl. Crystallogr.* **2** 65
[21] Rodriguez-Carvajal J 1993 *Physica* B **192** 55
[22] Mydosh J A 1993 *Spin Glasses* (London: Taylor and Francis)
   Maletta H and Zinn W 1989 *Handbook on the Physics and Chemistry of the Rare Earths* vol 12, ed K A Gschneidner Jr and L Eyring (Amsterdam: Elsevier Science) p 213
   Binder K and Young A P 1986 *Rev. Mod. Phys.* **58** 801
[23] Legvold S 1972 *Magnetic Properties of Rare Earth Metals* ed R J Elliott (London: Plenum) p 335
[24] Das I and Sampathkumaran E V 1994 *Phys. Rev.* B **49** 3972
[25] Malaman B, Venturini G, Blaise A, Sanchez J P and Amoretti G 1993 *Phys. Rev.* B **47** 8681